Comparison of Radar Reflectivity Calculations to Satellite Measurements Across the Melting Layer of Precipitation

Konstantinos Pipis, [1] ***Melina Ioannidou,*** [2] ***and Dimitrios Chrissoulidis***[3]

[1]Aristotle University of Thessaloniki, Department of Electrical & Computer Engineering,
GR-54124 Thessaloniki, Greece, email: konstantinos.pipis@gmail.com

[2] Alexander Technological Educational Institute of Thessaloniki, Department of Electronics,
GR-57400 Thessaloniki, Greece, tel.: +302310013616, fax: +302310791622, email: melina@el.teithe.gr

[3]Aristotle University of Thessaloniki, Department of Electrical & Computer Engineering,
GR-54124 Thessaloniki, Greece, tel.: +302310996334, fax: +302310994246, email: dpchriss@auth.gr

Abstract

Calculations of the radar reflectivity factor across the melting layer of precipitation successfully reproduce measured data provided by the Precipitation Radar (PR) of the Tropical Rainfall Measurement Mission (TRMM) satellite. This work proves that calculations made by use of a proposed modeling scheme, which is based on the eccentric spheres model for melting ice particles, deviate from measurements by no more than 8%. As a side effect of the comparisons made, cases of erroneous information about the height and width of the melting layer in TRMM data sets are brought to the light.

1. Introduction

Radio wave propagation through the melting layer of precipitation has drawn strong interest over the years. The melting layer extends from the $0^{\circ}C$ isotherm downwards, it is composed of ice or snow particles which gradually melt into falling raindrops, and it is associated with enhanced radar reflectivity, which is commonly referred to as *bright band*. We apply the eccentric spheres model to melting ice particles [1] and we calculate the radar reflectivity factor across the melting layer of precipitation by use of the hypothesis that melting begins at the top and ends at the bottom of that layer for all particles, which are considered non-interacting and non-uniform in size; the raindrops emerging from the bottom of the melting layer are assumed to follow the Marshall-Palmer (MP) or Gamma (G) size distribution. Numerical results obtained by use of this model are compared to measurements made by the Precipitation Radar (PR) of the Tropical Rainfall Measurement Mission (TRMM) satellite [2]. The boundaries of the melting layer are set in three ways. Numerical and measured data are plotted on the same chart for several rain rates in tropical and temperate zones. The efficiency of our theory in following reality is quantitatively assessed in every case.

2. Modelling of the Radar Reflectivity Across the Melting Layer

A melting ice particle is modeled as an ice sphere of radius α_2 eccentrically coated by a spherical water shell of radius α_1 (Fig. 1). The ice core shrinks as melting proceeds, but it is always at the top of the composite ice/water particle, because of gravity. Excitation by a plane electromagnetic wave, incident from the direction $\hat{i}$, is considered and the harmonic time dependence $e^{-j\omega t}$ is used. The scattering amplitude of any melting ice particle is given by [1]

$$\vec{f}^{\,t}\left(\hat{i},\hat{s}\right)=\frac{1}{k_0}\sum_{n=1}^{\infty}\sum_{m=-n}^{n}j^{-n}\left[\left(ma_{mn}^{t}\frac{P_n^m(\cos\theta)}{\sin\theta}+b_{mn}^{t}\frac{dP_n^m(\cos\theta)}{d\theta}\right)\hat{\theta}+j\left(mb_{mn}^{t}\frac{P_n^m(\cos\theta)}{\sin\theta}+a_{mn}^{t}\frac{dP_n^m(\cos\theta)}{d\theta}\right)\hat{\varphi}\right]e^{jm\varphi}\,, \qquad (1)$$

where $k_0=\omega\sqrt{\mu_0\varepsilon_0}$ is the wave-number in free space, the angles θ,φ define the scattering direction $\hat{s}$, $P_n^m(\cos\theta)$ is an associated Legendre function of the 1st kind, and a_{mn}^{t}, b_{mn}^{t} are the wave amplitudes of the scattered wave; the superscript $t=1,2$ implies that the incident wave is polarized along $\hat{e}_1=\hat{y}$ or $\hat{e}_2=-\hat{x}\cos\theta_{inc}+\hat{z}\sin\theta_{inc}$.

978-1-4244-6051-9/11/$26.00 ©2011 IEEE

The radar cross-section of a single, melting ice particle is given by $\sigma_b(\alpha_1) = 4\pi\left|\vec{f}^{\,t}\left(\hat{i},-\hat{i}\right)\right|^2$ and the radar cross-section per unit volume in the melting layer is determined by integration over all possible particle sizes:

$$\gamma_b(Q) = \int_{\alpha_{1,\min}}^{\alpha_{1,\max}} \sigma_b(\alpha_1) N(\alpha_1)\, d\alpha_1 = q \int_{\alpha_{\min}}^{\alpha_{\max}} \sigma_b(q\alpha) N(\alpha)\, d\alpha\,. \tag{2}$$

$N(\alpha_1)$ and $N(\alpha)$ in equation (2) are the size densities of melting ice particles and raindrops, respectively, i.e, the number of such particles per unit volume for any given size.

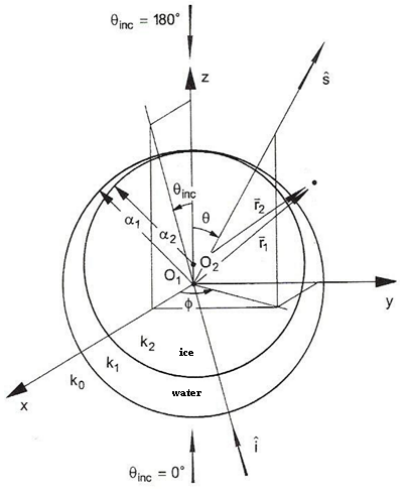

Fig. 1. Geometry of melting ice particle and scattering configuration

The outcome $\gamma_b(Q)$ is a function of the mass fraction $Q = m_w/m$, where m_w is the mass of melt water and m is the overall mass of any melting ice particle. Mass conservation links the radius α_1 of melting ice particles to the radius α of raindrops underneath the melting layer of precipitation by the simple equation $\alpha_1 = q\alpha$, wherein $q^3 = Q + \rho_w(1-Q)/\rho_i$ and ρ_w, ρ_i stand for the densities of water and ice. The size α of raindrops is assumed to vary in the range $[\alpha_{\min}, \alpha_{\max}] = [0.025, 0.325]$cm according to the MP or G size distribution [1]; both distributions involve the rain rate R, measured in mm / hr, as the key parameter which ultimately controls the mass density in the melting layer. The equivalent radar reflectivity factor in dBZ (Z in mm^6/m^3) is defined by [1]

$$Z_{eq}(Q) = 10\log_{10}\left[\frac{\lambda^4}{\pi^5}\left|\frac{n_w^2+2}{n_w^2-1}\right|^2 \gamma_b(Q)\right], \tag{3}$$

where λ (mm) is the wavelength and n_w is the (complex) refractive index of water. The position of a melting ice particle, relative to the top of the melting layer, is linked to the mass fraction Q through the equation $2Q = 1 + \sin(h\pi/H_{\max} - \pi/2)$ [3], where $0 \le h \le H_{\max}$ and $H_{\max}$ is the width of the melting layer. Thus, $Z_{eq}(Q)$ is transformed into $Z_{eq}(h)$, which is the end-result of our modelling scheme.

3. Positioning of the Melting Layer

Measurements of the radar reflectivity factor, subsequently denoted by $\hat{Z}_{eq}$, and of the rain rate have been obtained from Data Sets 1C21:*Radar Reflectivity*, 2A23:*Radar Rain Characteristics*, and 2A25:*Radar Rainfall Rate and Profile* of the TRMM Data Group *Orbital*; all those data have been acquired by the PR instrument, they are

stored as *.HDF files, HDF being shorthand for Hierarchical Data Format, and they can be downloaded from http://mirador.gsfc.nasa.gov/ by use of the software package HDFView. Comparison of $Z_{eq}(h)$ to $\hat{Z}_{eq}(h)$, the latter serving as reference, requires accurate positioning of the melting layer. Surprisingly, we have found several cases of absurd information in Data Set 2A23 about the bottom, top, and width of the melting layer. Hence, we have had three options to position the melting layer prior to comparing calculations to measurements.

The Max-RL method: The bottom of the melting layer is assumed to coincide with the maximum of $\hat{Z}_{eq}$, whereas the top is set by use of the formula $H_{\max} = 492R^{0.272}$, proposed by Russchenberg and Lighthart [3]. A comparison made in this way is shown in Fig. 2; calculations made by use of the MP/G distribution are shown by the red/green curve. The merit of calculations is assessed by use of $MSQE=\sqrt{M^{-1}\sum_{i=1}^{M}\left(Z_{eq}(h_i)-\hat{Z}_{eq}(h_i)\right)^2}$, i.e. a mean-square error with respect to measurements made at the heights h_i, $i=1,2,...,M$ which fall within the melting layer. The *MSQE* is 6.3% and 3.6% for the MP and G size distribution, respectively.

The Max-Data method: The bottom of the melting layer is set, again, as above, but the top is set by use of the value found in the aforesaid Data Set 2A23. A comparison made in this way is shown in Fig. 3; the *MSQE* is 3.1% and 5.8% in this case for the MP and G size distribution, respectively.

The Data-Data method: Both boundaries of the melting layer are retrieved from Data Set 2A23. Comparisons made in this way are shown in Fig.4; on the left a successful comparison is shown, whereas on the right the comparison has failed, obviously because of incorrect positioning of the melting layer in TRMM Data Group *Orbital*. Having examined more than 50 height profiles of $\hat{Z}_{eq}$, some over tropical and others over temperate regions, we have concluded that positioning of the melting layer by the *Data-Data* method is unreliable; hence, this method has been abandoned.

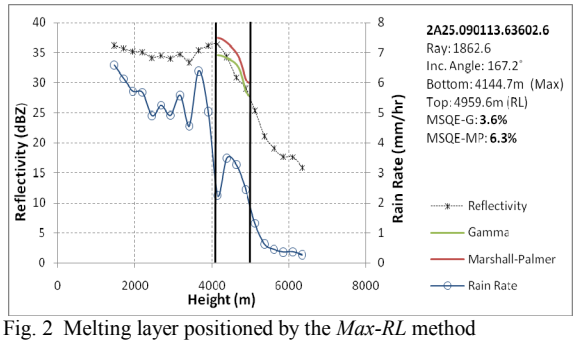

Fig. 2 Melting layer positioned by the *Max-RL* method

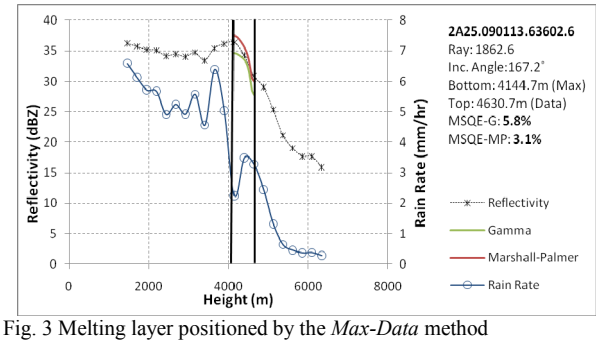

Fig. 3 Melting layer positioned by the *Max-Data* method

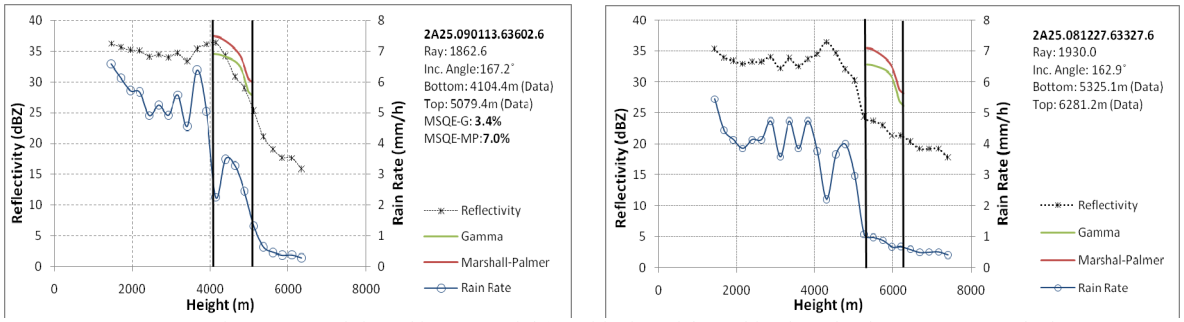

Fig. 4 Correct (left) and incorrect (right) positioning of the melting layer by the *Data-Data* method

4. Comparison of Calculations to Measurements

The average *MSQE* from all comparisons made over tropical and temperate regions is shown in Table I. The worst result arises over tropical regions with the melting layer positioned by the *Max-Data* method and the raindrops

G-distributed. If that combination is put aside, it can be said that (a) the *MSQE* is smaller in tropical than temperate regions, (b) the MP distribution favors our calculations more than the G distribution, and (c) neither the positioning method nor the size distribution have significant effect on the *MSQE* over temperate regions.

Table I. Mean-square error *MSQE* (%) of calculations

Max-RL Positioning				*Max-Data* Positioning			
Temperate Zone		Tropical Zone		Temperate Zone		Tropical Zone	
G	MP	G	MP	G	MP	G	MP
8,14	8,07	7,77	7,13	8,00	7,71	**8,54**	7,17

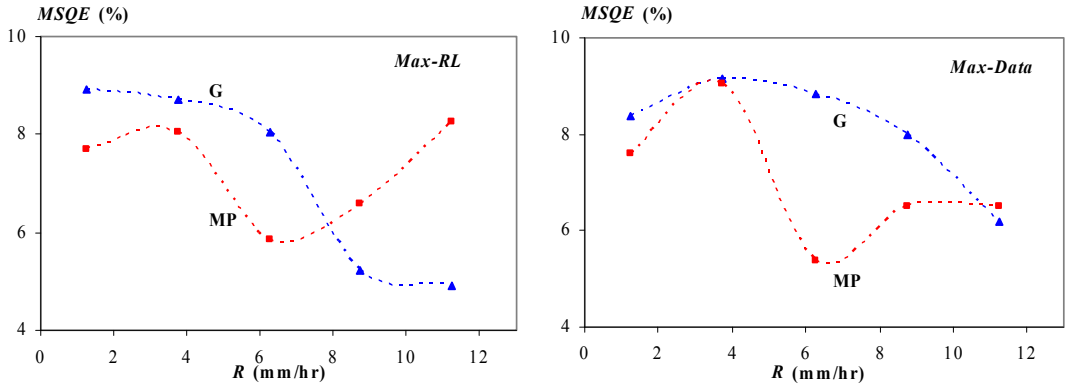

Fig. 5 *MSQE* of calculations versus rain rate; the melting layer has been positioned by the *Max-RL* (left) and the *Max-Data* method (right)

A glimpse into the effect of the rain rate *R* on the *MSQE* is offered by Fig. 5. As previously with the results of Table I, we notice from Fig. 5 that the MP distribution yields better results than the G distribution, unless the rain exceeds 8 mm / hr (*Max-RL* positioning) or 11 mm / hr (*Max-Data* positioning). Furthermore, we notice that, if the G distribution is used, the *MSQE* decreases as *R* increases; the minimum value of the *MSQE* is 5% and it occurs for *R* exceeding 10 mm / hr with the melting layer positioned by the *Max-RL* method. If the MP distribution is used, the *MSQE* is minimal (about 5%, too) for rain rates in the range 6-7 mm / hr with the melting layer positioned by the *Max-Data* method.

5. Conclusions

Simulations of the radar reflectivity factor across the melting layer of precipitation, made by use of the eccentric spheres model for melting ice particles, successfully follow measured data obtained by the PR instrument of the TRMM satellite; the mean-square error of our calculations can be as small as 5% on some occasions and it is about 8% on average. Comparisons of calculations to measurements have been made over tropical and temperate regions. Our calculations follow measurements best, if the raindrops are sized according to the Marshall-Palmer distribution and rain rates are low or if the raindrops follow the Gamma distribution and rain rates are high.

6. References

1. M.P. Ioannidou, D.I. Bakatsoula, and D.P. Chrissoulidis, "Scattering of radiowaves by melting ice particles: An eccentric spheres model," *J. Quant. Spectrosc. Radiat. Transf.*, **63**(2), Sep. 1999, pp. 585-597.

2. T. Kozu et al., "Development of precipitation radar onboard the tropical rainfall measuring mission (TRMM) satellite," *IEEE Trans. Geosci. Remote Sens.*, **39(1)**, Jan. 2001, pp. 102-116.

3. H.W. Russchenberg and L.P. Lighthart, "Backscattering by and propagation through the melting layer of precipitation: A new polarimetric model," *IEEE Trans. Geosci. Remote Sens.*, **34(1)**, Jan. 1996, pp. 3-14.